Color Properties of Specular Reflections

J.S. Arney, P.G. Anderson and William Pfeister
Rochester Institute of Technology
Rochester, New York, USA

Abstract

As part of a project to develop improved analytical techniques for the characterization of print gloss, a study has been carried out on the chromatic effects on specular reflections. Fresnel's reflection law suggests one kind of chromatic effect. An increase in index of refraction occurs in a material as the wavelength of light approaches the wavelength of absorption, and the increased index results in an increased Fresnel reflection. However, analysis of C, M, and Y electrophotographic images did not reveal any evidence of this effect. Another very strong effect was found to be the contribution of Fresnel type reflections from sub-layers of the image to the first surface reflection. These sub layer effects were observed to contribute significantly to the total specular reflectance, provided the colorant layer had a minimum absorptance. For example, for measurements of C, M, and Y toner fused on paper, measured in R, G, and B light, the minimum amount of specular reflection was measured for Cyan in Red, Magenta in Green, and Yellow in Blue. Quantitative modeling of this multiple specular reflection has been consistent with experimental measurements.

Introduction

It is useful to distinguish between the term "gloss" and the term "specular reflection". The former is used in this report to mean the visual attribute, and the latter refers to light measured instrumentally. The term "gloss" is intuitively familiar as a phenomenon that increases the color value and decreases the chroma of printed images. We do not generally associate gloss with hue or wavelength effects. However, instrumental measurements of specularly reflected light do show significant wavelengths effects.[1] This report describes measurements of these effects and suggests an optical model of specular reflection that may be useful in relating instrumental measurements both to material properties and to visual impressions of gloss.

Chromatic Aberration

Specular light reflected from a smooth surface is well known as Fresnel's law,[2] which says that the amount of reflected light is determined by, and only by, the indices of refraction of the materials at the surface. The refractive index of a material increases as the wavelength of light approaches an absorption band of the material; a phenomenon responsible for chromatic aberration in lenses and spectral dispersion in prisms. Fresnel's law tells us that an increase in the refractive index of an ink layer will increase the amount of specularly reflected light. Thus, one would expect to observe specular behavior in measurements of specular reflection. Indeed, a recent study by Granberg[1] reported a study of specular reflections from cyan and magenta inks and attributed observed differences to sharp increases in refractive index at the absorption peaks of the inks. As will be described below, attempts to reproduce this phenomenon with electrophotographic toners resulted in a very different kind of chromatic behavior.

The Measurement Technique

Figure 1 is a schematic illustration of the instrument used in the current work. Details of the instrument are described elsewhere, and a summery is given here.[3,4]

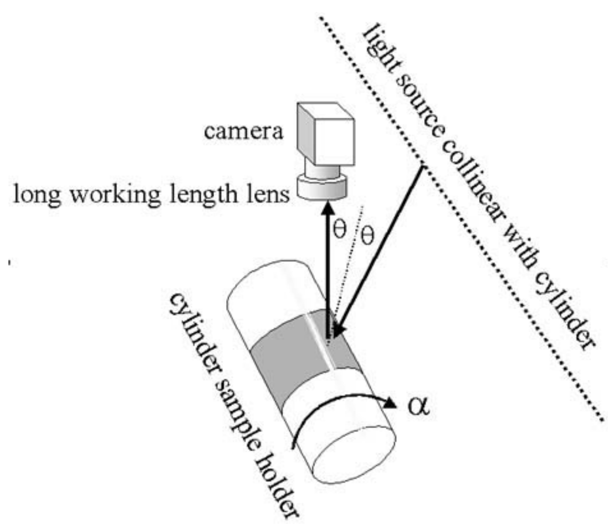

Figure 1. Schematic diagram of the instrument. A specular angle of $\theta = 20^o$ was used.[3,4]

The printed sample is wrapped around a cylinder and illuminated with a line source that is collinear with the cylinder. An electronic camera captures an image of the sample. The camera uses a lens with a long working distance so that parallax from one side of the sample to the other can be ignored. The line light source is sufficiently long and sufficiently far from the cylinder to approximate an infinitely long source at infinity. The light from the source is linearly polarized, and an analyzer is used in the front of the camera lens. Images are captured with parallel polarizers and crossed polarizers, and the difference image is produced. The difference image contains only that light which maintains polarization when it is reflected. The diffuse, bulk scattered light is thereby eliminated from the measurement.[5]

An illustration of an image captured with the micro-gonio-photometer is shown in Figure 2. The specular band is clearly visible, and its angular location, α, is calculated from the known geometry of the cylinder. A horizontal scan of this image produces a BDRF curve showing the specular lobe centered at α = 0, where α is the mean surface angle of the sample and is θ/2 from the angles of illumination and detection.

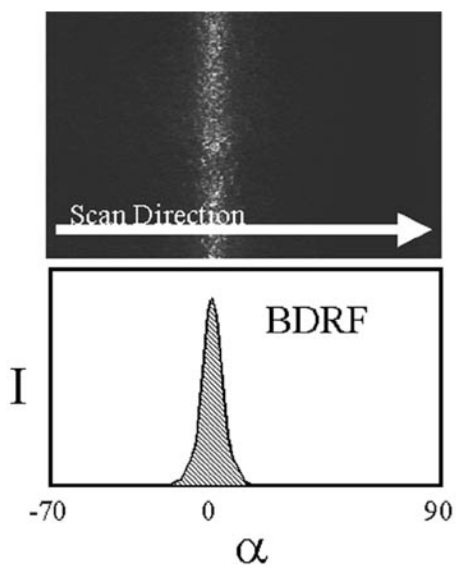

Figure 2. Illustration of an image and a BDRF from the device shown in Fig. 1.

The device illustrated in Fig. 1 produces a BDRF by varying the angle of the sample, α, rather than varying the angle of the source or the detector, as is more commonly done.[6-8] Surface roughness spreads the specular lobe out over some width in the α direction.[9,10] A complete BDRF analysis would measure the specular lobe in both orthogonal directions, α and the β. The approximation of an infinitely long light source averages the specular lobe in the β direction. In addition, by scanning the sample angle, α, instead of the source or detector angles, the equal/opposite Fresnel angle, θ, remains constant over the entire angular range of the BDRF. As a result, the shape of the specular lobe in Fig. 2 should be a function only of the topography of the sample, and the area under the lobe should be proportional to the total Fresnel reflectance. Experimental verification of this device has been described elsewhere.[3]

The Samples and the Data

Solid patches of cyan, of magenta, of yellow, and of process black were printed on non-coated, super calendered paper using an Indigo Ultrastream, liquid electrophotographic printer. The samples were mounted on the cylindrical sample holder, and measurements were made using light filtered through red, green, and blue filters (status A). Figure 3 shows the resulting BDRF curves for the cyan sample measured with red, green, and blue light.

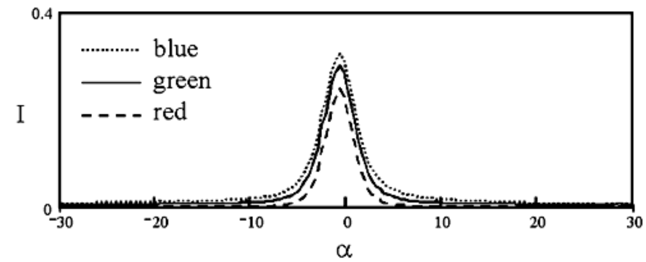

Figure 3. Micro-gonio-photometric BDRF curves measured for the cyan ink using red, green, and blue light.

Table I. Measured values of area, A, under the BDRF curve for cyan, magenta, and yellow ink measured with red, green, and blue light. Areas at each source color are expressed relative to the area of the process black.

ink source	Cyan	Magenta	Yellow	Black CMY
Red	1.2	1.7	1.4	1.00
Green	1.4	1.2	1.3	1.00
Blue	1.5	1.2	1.0	1.00

The BDRF curves for cyan shown in Figure 3 differ significantly in red, green, and blue light. Peak height, pick width, and area are all different. The peak height and the area both increase in the order red, green, blue. This indicates that the amount of Fresnel reflected light is greatest for blue light and least for red light. Similar measurements were made for solid printed samples of magenta and yellow. Table I summarizes the results of measurements of the total area, A, of the BDRF curves for the cyan, magenta, yellow, and process black.

The Optical Dispersion Model

The areas shown in Table I are expressed relative to the process black (C+M+Y) where the areas of the black are defined as 1.00 for red, green, and blue light. The data in Table I show a significant wavelength effect. The light that shows the least specular reflectance is the light that is most strongly absorbed by the ink. For example, red light on cyan ink and blue light on yellow ink show low specular reflectance. These measurements

Because of the way the instrument was configured, the differences in the areas in Table I can not be rationalized as differences in topographic roughness or Fresnel specular angle, θ. A rational consistent with Fresnel's law is needed.

As discussed earlier, Grandberg recently suggested a model to account for wavelength effects on Fresnel reflectance.[1] That model is based on a wavelength-dependent index of refraction. This effect is well known and is the cause of optical wavelength dispersion in a prism. This optical dispersion model, however, predicts that the wavelength most strongly absorbed by the ink should produce the highest specular reflectance. The observations summarized in Table I behave in exactly the opposite way. Additional measurements made with images printed with solid C, M, and Y patches of dry electrophotographic toner, and samples of colored glass were measured less quantitatively than the samples of Table I, but the trend of higher specular reflectance at lower optical density was also observed for those materials. This suggests that the matrix binder of the colorant, rather than the colorant material itself, is the material primarily responsible for the system index and the specular reflectance. Since the matrix binder is nearly colorless, the index is not significantly dependent on wavelength. However, this does not explain the significant decrease in specular light at wavelengths of strong absorption.

The Two Layer Model

Figure 4 shows a model of specular reflectance in which light is specularly reflected both from the air/ink interface and from the ink/paper interface. Fresnel's law and the index of refraction of common organic materials suggests a Fresnel reflectance factor of $\rho_1 \cong 0.04$ (4%) at the air/ink interface. Most of the light $(1 - \rho_1)$ continues into the ink layer. If the ink layer strongly absorbs this light, it does not contribute to the measured specular reflection. However, if the ink does not absorb the light (blue light with cyan ink, for example), then the light encounters the ink/paper interface. A significant reflectance at this second interface, ρ_2, would result in a significant contribution to the overall specular light reflected from the ink. Qualitatively, this would rationalize the observations in Table I.

The two layer model rationalizes the general trends in Table I, but a quantitative estimate of the second specular reflectance, ρ_2, suggests this model is not complete. The index of refraction difference between air and ink is approximately 0.4 to 0.5, and this results in $\rho_1 \cong 0.04$ according to Fresnel's law. However, the index difference between ink and paper is not likely to be more than about 0.1. This would result in $\rho_2 \cong 0.001$, which is only about 2% of the value of ρ_1. In other words, the second layer model of Figure 4 is not able to rationalize the magnitude differences observed in Table I.

The Air-Gap Model

In order to rationalize the magnitude differences in Table I with a multi-layer model, a large index difference is required at the layers. We can rationalize a large index difference at the second layer, ρ_2, if we assume an air gap between the ink and the paper as illustrated in Figure 5. In addition, an air gap would result in a third layer, ρ_3, with a large index difference between air and paper. The total specular light would be the sum $I_1 + I_2 + I_3$. Note that I_2 and I_3 are governed by the transmittance of the ink, T, as well as by Fresnel's law. This model can rationalize both the order and the magnitude of the observations summarized in Table I.

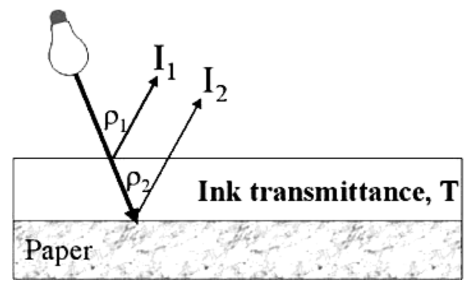

Figure 4. A model of specular reflectance based on reflection from two interfaces

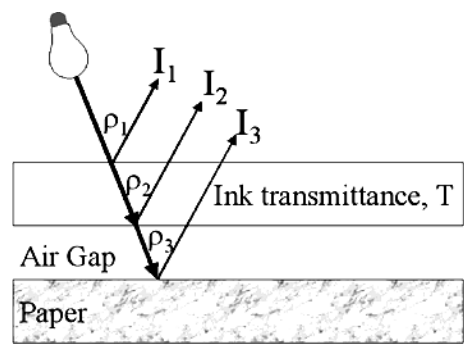

Figure 5. Air-gap model of specular reflectance

The air-gap model is not a model that assumes ink is floating above the paper. Rather, one can imagine that the ink does not completely wet the paper surface. This would result in less than a perfect optical coupling between the ink and the paper, which would mean at least a mono molecular layer of air between the ink and the paper, and Fresnel type reflections from the three layers illustrated in Figure 5.

Quantitative Test of the Model

The model shown in Figure 5 can be expressed quantitatively by adding up the contributions of the three reflections. Equations 1 and 2 are the net reflectance one would expect from the two layer model. R_n is the no-air-gap model, and R_a is the air-gap model. We distinguish between the two value $\rho_2 = \rho_{2n}$ and $\rho_2 = \rho_{2a}$.

$$R_n = \rho_1 + T^2 \cdot (1 - \rho_1)^2 \cdot \rho_{2n} \quad (1)$$

$$R_a = \rho_1 + T^2 \cdot (1 - \rho_1)^2 \cdot \rho_{2n} + T^2 \cdot (1 - \rho_1)^2 \cdot \cdot (1 - \rho_{2a})^2 \rho_3 \quad (2)$$

In order to test equations (1) and (2), values of ink transmittance are needed. These were estimated from optical measurements of ink reflectance made with 45°/ 0° geometry using status A filters. Transmittance values, T, were calculated with equation (3) where R and R_g are the measured ink and background paper reflectance respectively. The resulting estimates of T are shown in Table II, and the correlation between area, A, and squared transmittance, T^2, is shown in Figure 6.

$$T = (R/R_g)^{1/2} \quad (3)$$

Table II. Measured values of ink transmittance, T, for printed samples of cyan, magenta, and yellow ink measured red, green, and blue light.

ink source	Cyan	Magenta	Yellow	Black CMY
Red	0.18	0.94	0.89	0.10
Green	0.63	0.18	0.84	0.10
Blue	0.82	0.49	0.23	0.10

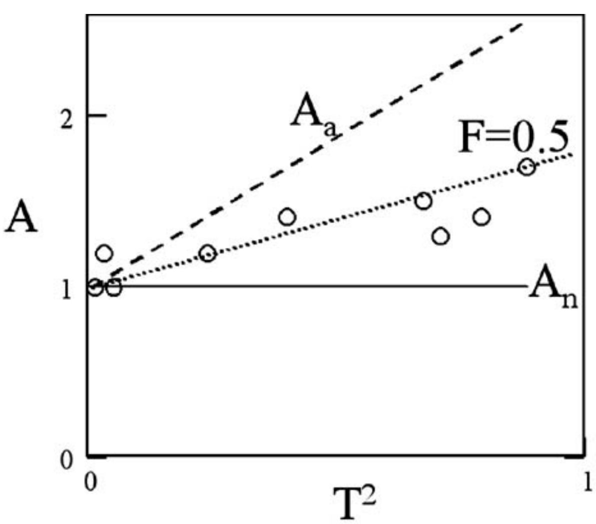

Figure 6. Gonio-photometric peak areas, A, versus the square of the ink transmittance values, T^2, for the solid ink samples printed on calendered paper with an Indigo Ultrastream printer. The lines A_a, A_n and F are described in the text.

A value of $T^2 = 0.01$ is estimated for the process (CMY) black. This value is approximately zero, so the value of $R_n = R_a = \rho_1$ for the process black at red, green, and blue. This leads to the following models for the relative area of the specular lobes in Table I. If we make the approximations $\rho_{2n} = 0$ and $\rho_1 = \rho_{2a}, = \rho_3$, then we can model the data shown in Figure 6 with equations (4) and (5).

$$A_n = 1 \quad (4)$$

$$A_a = 1 + T^2 \cdot (1-\rho_1)^2 \cdot [1 + (1-\rho_1)^2] \quad (5)$$

The solid line labeled A_n in Figure 6 is equation (4), and the dashed line labeled A_a is equation (5) with $\rho_1 = 0.04$. The dotted line labeled F in Figure 6 can be modeled with equation (5) only if $\rho_1 = 0.30$. This would require an ink index of refraction of n = 3.4, which is an absurdly high value. Alternatively, we might assume that the ink partially wets the substrate paper to produce a fraction of interface that is optically coupled and a fraction not optically coupled. This is described by equation (6) with a gap area fraction of F = 0.5, and this equation rationalizes the dotted line in Figure 6.

$$A = F \cdot A_a + (1-F) \cdot A_n \quad (6)$$

Discussion

The effect of wavelength on specular reflectance from a printed surface is experimentally quite significant. The most transparent ink/light combination in this study was found to reflect nearly twice as much as highly absorbing inks. The proposed model of specular reflection from an ink image involves specular reflections from more than one layer. This does rationalize the qualitative observations of decreased specular reflectance with increased ink absorption. This model also rationalizes the linear relationship between measured values of A and T^2. However, in order to fit the experimental data quantitatively, the model requires a fraction parameter, $0 < F < 1$. This is imagined to represent a fractional area of the ink/paper interface that is not optically coupled. No independent evidence has yet been obtained to support this supposition, and further research is underway to investigate this model.

References

The authors would like to express appreciation to Hewlett-Packard Corporation for grant support of this project.

Acknowledgements

1. Hjalmar, Granberg Paper Optics and Perception: Spectral Light Absorption and Gloss of Cyan & Magenta Inks, Acreo Tryckteknisk Forskning, Report No. acr009805, Norrköping, SE, Dec. 2002.
2. F. A. Jenkins and H.E. White, Fundamentals of Optics.

3. J. S. Arney, H. Hoon, and P. G. Anderson, A Micro-Goniophotometer and the Measurement of Print Gloss, J. Imag. Sci. & Technol., in press 48:(2003).
4. J. S. Arney and Hung Tran, An Inexpensive Micro-Goniophotometry You Can Build, Proc. PICS, pg. 179 (1998).
5. J. S. Arney, Klaus Pollmeier, and J. Michel, Technique for Analysis of Surface Topography of Photographic Prints by Spatial Analysis of First Surface Reflectance, J. Imag. Sci. & Technol., 46(4): 350 (2002).
6. Standard Practice for Angle Resolved Optical Scatter Measurements on Specular or Diffuse Surfaces, Standard Procedure No. E 1392-96, American Society for Testing and Materials, 1996.
7. I. Nimeroff, Analysis of Goniophotometric Reflection Curves, J. of Research of the Nat. Bureau of Std., 48(6): (1952).
8. I. Nimeroff, Two-parameter Gloss Methods, J. Research of the Nat. Bureau of std., 58(3): 127(1957).
9. H. Rothe and D. Huester, Application of Circular and Spherical Statistics for the Interpretation of BDRF Measurements, Scattering and Surface Roughness, SPIE Vol. 3141-02, p.13 (1997).
10. M. A. MacGregor and P. Å. Johansson, Submillimeter Gloss Variations in Coated Paper, Part 1, TAPPI. **73**(12): 161 (1990), and Part 2, TAPPI **74**(1): 187(1991).

Biography

Jon Arney is Associate Professor in Imaging Science at Rochester Institute of Technology where he teaches courses in tone and color reproduction, and image microstructure. He is faculty advisor for the Student Chapter of IS&T and for the RIT Amateur Radio Club (K2GXT). Jon's research focuses on the optical properties of ink and paper. Current work involves the development models of laser EP tone reproduction and noise characteristics that are independent of the chosen halftone screen. The calibrated model is used in conjunction with computer search algorithms to optimize the calibrated printer. Another project involves a detailed study of gloss in which the optical microstructure of the gloss reflection is measured and understood quantitatively. This has lead to the development of micro-gloss instrumentation and theoretical models to describe gloss. The focus is on understanding gloss and extracting appropriate experimental metrics capable of correlating with visual perception of gloss. Jon is an active member of IS&T and publishes regularly in the journals and proceedings of that organization.